AD NUMBER

AD010920

NEW LIMITATION CHANGE

TO

Approved for public release, distribution unlimited

FROM

Distribution authorized to U.S. Gov't. agencies and their contractors; Administrative/Operational Use; JAN 1953. Other requests shall be referred to Office of Naval Research, Arlington, VA.

AUTHORITY

onr ltr, 26 oct 1977

AD-

10920

THE OHIO STATE UNIVERSITY
RESEARCH FOUNDATION

Technical Report No. 2
RF Project 355

R E P O R T

by

THE OHIO STATE UNIVERSITY
RESEARCH FOUNDATION

Columbus 10, Ohio

Cooperator: OFFICE OF NAVAL RESEARCH, NAVY DEPARTMENT
N6onr 225-17 NR 017 408

Investigation of: ORDER-DISORDER TRANSFORMATIONS IN CRYSTALS

Subject of Report: Amplitudes of Vibration and X-ray Scattering of Crystalline Lithium Hydride and Lithium Deuteride: 300°K to 20°K

Submitted by: C. K. Stambaugh and P. M. Harris

Date: January 1953

CONTENTS

SUMMARY

1. Intensities of Laue-Bragg scattering from powdered crystals of LiH and LiD were obtained at four temperatures, 20°K, 77°K, 194°K, and 303°K, using a recording G-M counter spectrometer and a special dewar specimen mount.

2. Relative crystal structure factors, F_{rel} and relative atomic form factors were calculated from the intensities.

3. Absolute atomic form factors were obtained from the relative values by use of independent data.

4. Characteristic temperatures, Θ, for LiH and LiD were obtained from the relative form factor data.

5. Temperature coefficients, B_t, and amplitudes of vibration, $\sqrt{\overline{\mu^2}}$, were calculated from the Θ values.

6. Electron density distributions, ρ_{xoo}, were obtained for LiH from the absolute atomic form factor data.

7. Radial charge distributions, U(r), were calculated from the ρ_{xoo}.

8. Evidence suggestive of a change in the state of ionization of the crystals with changes in temperature was found.

AMPLITUDES OF VIBRATION AND X-RAY SCATTERING OF CRYSTALLINE LITHIUM HYDRIDE AND LITHIUM DEUTERIDE: 300°K TO 20°K

P. M. Harris C. K. Stambaugh*

1. INTRODUCTION

This investigation of lithium hydride and lithium deuteride was begun through interest in the thermal vibrations and distribution of charge in the crystal. Since force constants and bonding in LiD are presumably the same as in LiH, experimentally observed differences in the scattering powers of the atoms or ions of the lattices of LiH and LiD for x-rays should arise solely from the mass change. Also, such effects in this case should be the largest observable, since the fractional change in mass is the largest possible and the fraction of total charge contributing to bonding, whatever the type, is also large.

A number of investigators have made photographic studies of the Laue-Bragg diffraction of LiH. (1-6) All are in agreement with a polar, NaCl-type lattice of Li^+, H^- ions. Ubbelohde (7) discussed the difference in cell size of LiH and LiD, attributing it to a difference in zero point energy. Lonsdale (8) calculated amplitudes of vibration of the atoms in LiH and LiD using Ubbelohde's characteristic temperatures and a mean atomic weight. Except for the qualitative investigation by Bijvoet and Frederikse (4) the only experimental observation of the effect of thermal vibration on the intensities of the diffraction maxima from LiH was that of Griffith (9). Recently Ahmed (10) has published certain other results which will be discussed.

* Major, U.S.A.F., now at AIR RESEARCH LABORATORY, CAMBRIDGE, MASS.

2. EXPERIMENTAL

APPARATUS

The intensity of scattering of x-rays from powdered samples of the hydride and deuteride at the Bragg angles was measured by means of a G-M counter-spectrometer. The spectrometer was that described by Van Horn[11], except that a G-M counter tube was substituted for the ionization chamber and a synchronous motor was attached to the worm gear drive. The G-M tube was a North American Philips number 62003, with a thin mica window. The pulses from the tube were integrated and transmitted as a counting rate by a General Radio type 1500A counting-rate meter, the output of which was continuously recorded by a Brown recorder. In order to have the time scale of the recorder chart read in degrees and minutes of chamber angle, the motor drive of the spectrometer was synchronized with the chart drive.

For calibration purposes a Tracerlab 3C1A Autoscaler was used with the same G-M tube, and with the spectrometer turned by hand to fixed positions.

The x-ray source was a Machlett copper target type A-2 tube, with the primary beam filtered by nickel foil sufficiently thick to reduce the Cu Kβ to less than one per cent of its unfiltered value. The high voltage, approximately thirty-five kilovolts, was supplied by an oil-immersed high voltage transformer and full wave rectifier unit. The power supply for this unit was a war surplus four hundred cycle generator, belt driven by three one-horsepower electric motors.

To stabilize the anode current of the x-ray tube the circuit of Figure 1 was used. Fluctuations of plate current were detected and amplified by the right hand portion of the circuit, as shown. This amplified signal produced a change in the conductance of the 6B4 tubes, causing in turn a variation of the impedance of the transformer on the left (used as a saturable reactor), thus changing the filament current of the x-ray tube. Random variation of the anode current was reduced by this means to about three per cent.

All data on the intensity of scattering of x-rays were obtained using transmission through a compacted powder-rod mounted in a modification of the dewar described by Griffith[9]. Figure 2 is a sectional view of the modified dewar. The specimen-rods, one-eighth inch in diameter by one-half inch in length, were mounted in brass blocks so designed that the beam could completely bathe the cross section of the sample without striking the brass. These blocks were located in good thermal contact with the copper wall of the coolant reservoir. The x-ray beam entered and left the dewar chamber through plastic windows. Thermocouples were sunk in wells at the top and bottom of each brass block, as close as possible to the sample ends. Thin monel tubing supported the inner portion of the dewar in order to reduce heat leak to the coolant reservoir. The space between the outer wall and the reservoir and sample mount was continuously evacuated. Insulation and thermal shielding were sufficiently good that during the runs at twenty degrees Kelvin the loss of liquid hydrogen was about one hundred milliliters

per hour. The dewar was supported, with its axis coinciding with that of the spectrometer, by a cantilever mount.

Provision was made for mounting a sample each of lithium hydride and lithium deuteride, one above the other, in the dewar, to permit a direct comparison of the intensities of scattering of the two samples at chosen temperatures by a vertical displacement of the dewar.

PREPARATION OF SAMPLES

For this research there were available lithium hydride prepared by both Maywood Chemical Company and by Metal Hydrides, and lithium deuteride prepared by Metal Hydrides from deuteride allocated by Oak Ridge National Laboratory. Of the hydride preparations the former was the more pure and was used for all runs.

The crystalline material was ground to pass a four hundred mesh sieve and compacted in a dry box under an atmosphere of dry nitrogen, the drying of which was accomplished by means of a train composed of columns of Drierite, phosphorous pentoxide, and lithium hydride, in that order. The third column was provided to remove any additional impurities which might react with lithium hydride. In order to determine the extent of reaction of nitrogen with lithium hydride, heavily overexposed Debye patterns were obtained from samples which had remained in the nitrogen atmosphere for the duration of a usual sample preparation. No evidence of lithium nitride was found; however, small amounts of lithium hydroxide were detected.

The specimen was briquetted by means of the jig illustrated in Figure 3. The two halves of the die in the upper left portion of the drawing were pressed together to form a cylindrical cavity one-eighth inch in diameter. This die was clamped in the U-shaped portion of the vise with the cavity parallel to the arms of the U. Screws in one arm of the vise held the die firmly closed. The four-hundred mesh powder was packed into the cavity by use of an eighth-inch steel dowel-pin forced in by the screw in the remaining part of the vise.

The finished specimens were measured, and then weighed in sealed weighing bottles containing the dry nitrogen atmosphere, all weights being corrected for bouyancy. They were then returned to the dry box, where they were placed in the dewar specimen mount, which was then sealed and transferred to the spectrometer and immediately evacuated.

MEASUREMENT OF TEMPERATURE

The thermocouples mentioned in the description of the dewar specimen-mount were used to determine the temperature of the samples during the various runs. Due to evidence of unreliability of these thermocouple temperatures - especially at the lower temperatures at which calibration was obtained by extrapolation - the shift in Bragg θ due to thermal contraction was used as an additional check on sample temperature.

From combined thermocouple and thermal expansion data it is evident that the sample temperature did not differ by more than 10° from the

bath temperature. As a result, for the purposes of calculation, the sample temperature has been taken as the normal boiling point of the bath used, since the intensities of Bragg scattering are not very temperature-sensitive.

3. REDUCTION OF DATA

In the experimental operation the Brown recorder was so balanced that a chart reading of zero corresponded to an arbitrary counting rate slightly less than the lowest expected background, while full scale deflection corresponded to a counting rate slightly greater than the highest expected reading. The balance was different for each run. Since the balancing circuit was such that the relation of counting rate to chart reading was linear, calibration could be accomplished by determining counting rates at selected points with the auto-scaler.

If N is the counting rate at any chosen counter angle, and x is the chart reading at this angle, the relation is:

$$N = \alpha x + \beta, \qquad (1)$$

where α and β are constants for a given run, but may differ between runs. In order to determine α and β, the data for the strongest line of each run were used. The area under the curve for any peak is:

$$A_L = \int_{\phi_1}^{\phi_2} N d\phi = \alpha \int_{\phi_1}^{\phi_2} x d\phi + \beta \int_{\phi_1}^{\phi_2} d\phi$$

$$= \alpha A_x + \beta(\phi_2 - \phi_1), \qquad (2)$$

where A_L is the area in counts per second, A_x is the area in chart units,

ϕ is the angular setting of the counter (i.e., the Bragg angle 2θ), and ϕ_2 and ϕ_1 are the upper and lower angular limits of the peak.

If an arbitrary base line is selected, with end points N_1 and N_2 (or X_1 and X_2 on the chart) the area under this line is:

$$\begin{aligned} A_B &= \tfrac{1}{2} (\phi_2 - \phi_1) (N_2 + N_1) \\ &= \tfrac{1}{2} (\phi_2 - \phi_1) (\alpha x_2 + \beta + \alpha x_1 + \beta) \qquad (3) \\ &= \alpha A_{Bx} + \beta (\phi_2 - \phi_1), \end{aligned}$$

where A_{Bx} is the area under the line in chart units.

Then the net area between peak and base line is:

$$A_{net} = A_L - A_B = \alpha(A_x - A_{Bx}). \qquad (4)$$

Thus the ratio of the net area obtained from auto-scaler data to the net area obtained from the chart gives the scaling factor α. Substitution of A_L from scaler data, A_x from the chart, and α as determined above into equation (2) gives the additive constant β. The total areas for both chart data and auto-scaler data were evaluated using Simpson's one-third rule.

The values of α and β obtained in this manner compare favorably with those obtained by fitting scaler and chart data by the method of least squares, and are much more easily calculated. The agreement of scaler counting rates, converted to chart units by the inverse of equation (1), with the corresponding values on the charts is well within experimental error.

The observed counting rates as determined from the recorder charts by use of equation (1) are not true counting rates because of counts missed by the finite dead time of the G-M tube. According to Kurbatov and Mann,[12] for a random source of radiation, the correction for dead time takes the form:

$$Nc = N/(1 - \tau N), \tag{5}$$

where N is the observed counting rate, τ the dead time, and Nc is the corrected counting rate.

For a pulsating source of radiation, such as the emission from an x-ray tube with rectified high voltage, the correction is similar, according to investigations by Alexander, Kummer and Klug,[13] and by Cochran, [14] having in place of τ an effective dead time ϵ which is characteristic of the wave form of the source and the normal dead time of the counter.

The value of ϵ was determined experimentally by the following method. With the x-ray source operating in its usual condition and the G-M tube set at a position to receive radiation of not too great an intensity the following four readings were taken:

N_1 --- No absorber in the beam

N_2 --- One absorber in the beam

N_3 --- First absorber removed and second placed in the beam

N_4 --- Both absorbers in the beam

The corrected values of these counting rates have the relations:

$$\begin{aligned} Nc_2 &= Nc_1 \exp - \mu_1 x_1 \\ Nc_3 &= Nc_1 \exp - \mu_2 x_2 \\ Nc_4 &= Nc_1 \exp - (\mu_1 x_1 + \mu_2 x_2) \\ &= Nc_3 \exp - \mu_1 x_1 \\ Nc_2/Nc_1 &= Nc_4/Nc_3, \end{aligned} \qquad (6)$$

where μ_i is the linear absorbtion coefficient of the "i" the absorber and x_i is its thickness.

Substitution of the modified equation (5) into equation (6) gives for the effective dead time:

$$\epsilon = \frac{N_2N_3 - N_1N_4}{N_2N_3\,(N_1 + N_4) - N_1N_4\,(N_2 + N_3)} \quad . \qquad (7)$$

By this means ϵ (average) was found to be 4.52×10^{-4} sec.

After calibration of the charts by use of equation (1), values of counting rates were read from them at twenty-minute intervals of ϕ. These were corrected for dead time by equation (5) and the experimentally determined ϵ.

In order to facilitate drawing the base line, the corrected counting rates were multiplied by the corresponding reciprocal Lorentz and polarization factors ($\sin\theta \sin 2\theta / (1 + \cos^2 2\theta)$) and the results plotted against 2θ.

Since Nc is the intensity of radiation entering the counter at a given angle, the net areas under the peaks on these plots are proportional to $j\,|F|^2$, as can be seen by an examination of the expression for the power diffracted into the counter by a crystalline powder[15]:

$$P_d = P_o \frac{he^4 \lambda^3 M^2}{16 \pi r A m^2 c^4} \cdot \frac{1 + \cos^2 2\theta}{\sin \theta \sin 2\theta} \; j \, |F|^2 \delta V, \qquad (8)$$

in which:

P_d = power diffracted into the G-M counter

P_o = power per unit area in the primary beam

e = electronic charge

m = electronic mass

c = velocity of light

M = number of unit cells per unit volume

λ = wave length of x-rays

h = height of counter slit

r = distance from sample to geiger counter

A = area of slit limiting primary beam

2θ = angle between incident and diffracted beam

j = multiplicity, i.e. number of planes of like spacing

δV = effective volume

F = crystal structure factor, per unit cell, i.e.:

$$F = \sum_s f_s \exp \left\{-2\pi i \left(hx_s + ky_s + \ell z_s\right)\right\}, \qquad (9)$$

where summation is over all atoms of the unit cell

f_s = atomic form factor for atom "s"

h,k,ℓ = Miller indices of reflecting plane

x,y,z = coordinates of atoms in fractions of cell edge

The atomic form factor is independent of the wave length of the incident radiation only if the latter is sufficiently different from that of the absorption edge of the scattering atoms. This condition was fulfilled for lithium hydride and lithium deuteride.

From the plots as well as from the original charts, it was evident that in addition to lithium hydride* there was other diffracting matter

* Unless otherwise stated, whereever the words lithium hydride are used it is to be understood that the equivalent is true for lithium deuteride.

present. An investigation showed that all but a few of the extra peaks were due to the presence of lithium hydroxide. Unidentified weak lines were found at 67°30', 109°00', 113°00', 118°20', and 134°20'. They are presumed not to arise from the lithium hydride phase.

The effect of the impurities was to complicate the drawing of the base lines, since at most angles some scattering due to the LiCH or the unknown scatterer was superimposed on the background. However, it was believed that in the region between the LiH (111) and LiH (200) and between the LiOH (201) and LiH (220) the base line could properly be drawn tangent to the data curve, since no overlap was evident. With this as a point of departure, by repeated trial and error the base lines were drawn so that the areas under the hydroxide peaks were proportional to the values for $j|F|^2$ calculated for LiCH from data found in Crystal Structures[16].

It was discovered that each peak (lithium hydride and impurity alike) was distorted on the low angle side. If each peak was drawn symmetrically about the maximum, assuming the high angle side to be correct, then there remained a contribution on the low angle side which corresponded to a smaller peak one-tenth the height of, and one and one-half degrees away

from, the maximum of the peak it accompanied. These relations led to the conclusion that this distortion was actually a part of the peak and should be included in finding the area.

Resolution of overlapping peaks was carried out by trial and error, with the condition that close neighbors have the same shape. At the same time, correction for small peaks corresponding to the absorption edge of the nickel filter was made.

Ordinates of the curve for each peak were read at fifteen minute intervals, and the area under the curve found by Simpson's rule. The net area, or corrected "integrated intensity"

$$I' = k_j |F|^2 \tag{10}$$

was found by subtracting the area under the base line. Results are shown in Tables 1 a and 1 b.

Before correction for absorption in the sample could be made, it was necessary to determine the amount of lithium hydroxide present. This was accomplished for each run by comparing a LiOH and a LiH line chosen sufficiently close together that the absorption correction was the same for both.

The ratio of the "integrated intensities" of the two peaks chosen is:

$$\frac{I_1'}{I_2'} = \frac{k_1}{k_2} \frac{(j|F|^2)_1}{(j|F|^2)_2} \quad . \tag{11}$$

TABLE 1a. EXPERIMENTAL INTENSITIES FOR LiH

(Corrected for Lorentz and Polarization factors)

h k l	Temp., °K			
	20	77	194	303
111	479	950	360	883
200	1558	2626	1300	2792
220	1698	2692	1448	2705
311	1516	2705	1131	2662
222	721	1274	692	1192
400	599	729	568	759
331	923	1613	1178	1498
420	1165	1882	1128	1620
422	686	1102	542	930
121 (LiOH)	1500	995	1660	1020

TABLE 1b. EXPERIMENTAL INTENSITIES FOR LiD

(Corrected for Lorentz and Polarization factors)

h k l	Temp., °K			
	20	77	194	303
111	521	1582	1498	1766
200	1399	4397	4410	4801
220	1455	4396	4522	4623
311	1407	4271	3574	4293
222	748	2241	1781	1831
400	372	1121	823	995
331	767	2303	1856	2035
420	935	2883	2292	2152
422	561	1633	1240	1137

From equation (8) the expression for the constant for each substance is:

$$k_j = P_o \frac{he^4 \lambda^3}{16\pi r A m^2 c^4} M_j^2 \delta V = kM_j^2. \qquad (12)$$

Substituting in (11) and rearranging:

$$\left(\frac{M_1}{M_2}\right)^2 = \left(\frac{I_1}{I_2}\right) \frac{(j|F|^2)_2}{(j|F|^2)_1} \quad . \qquad (13)$$

The ratio of the weights of the two substances is:

$$\frac{W_1}{W_2} = \frac{d_1 M_1}{d_2 M_2} \quad , \qquad (14)$$

where d is the weight per unit cell.

Thus the weight fraction (x_1) is :

$$x_1 = \frac{W_1}{W_2} \Big/ \left(1 + \frac{W_1}{W_2}\right) \cdot \qquad (15)$$

The two lines chosen were LiOH (121) and LiH (220). Approximate values for f_{Li}, f_H, and f_{OH} were used, giving:

$\|F_1\| = 6.47$	$j = 16$	$(j\|F\|^2)_1 = 669.5$
$\|F_2\| = 2.5$	$j = 12$	$(j\|F\|^2)_2 = 75.0$

The results of calculations are shown in Table 2.

TABLE 2. WEIGHT FRACTION OF LiOH CONTAINED IN SAMPLES

Sample	Temp., °K			
	20	77	194	303
Li H	.32	.23	.35	.24
Li D	.30	.13	.12	.12

For the mixed sample the mass absorption coefficient is:

$$(\mu/\rho) = \left\{x_{LiH}(\mu/\rho)_{LiH} + x_{LiOH}(\mu/\rho)_{LiOH}\right\} = x_1\left\{(\mu/\rho)_{LiOH} - (\mu/\rho)_{LiH}\right\} + (\mu/\rho)_{LiH} \quad (16)$$

Griffith[9] found experimentally that the mass absorption coefficient for LiH was 0.74. Using this and the known value 12.7 for oxygen,[17] the coefficient for LiOH can be calculated, and in turn that for the sample. The latter is:

$$\mu/\rho = 8.73x_1 + .74 \quad (17)$$

With this equation, and using the measured values of ρ the density and R (the radius) for each sample the value of μR was found. These are shown in Table 3. With the latter, by interpolation in the proper tables[18] for Θ and for μR, the value of A, the absorption correction, was obtained for each peak.

The "intensities", corrected for multiplicity and absorption, can be expressed by:

$$I''_{(T,hkl)} = C_T^2 \left|F_{(T,hkl)}\right|^2 , \quad (18)$$

where the subscript T implies that C_T need not be the same for all runs. The difference in density would cause a small variation in C_T; however

it is probable that the greatest contribution to this variation would come from differences in the intensity of the primary beam.

TABLE 3. QUANTITIES USED IN DETERMINING ABSORPTION CORRECTIONS FOR THE SAMPLES OF LiH AND LiD

Symbol*	LiD				LiH			
	Temp., °K				Temp., °K			
	20	77	194	303	20	77	194	303
X_1	0.30	0.13	0.12	0.12	0.32	0.23	0.35	0.24
W_e	.07154	.07057	.07057	.07057	.06702	.06770	.07621	.06770
V_z	.0913	.0921	.0921	.0921	.104	.144	.107	.114
D	0.784	0.766	0.766	0.766	0.644	0.594	0.712	0.594
μ	2.63	1.44	1.37	1.37	2.28	1.63	2.71	1.68
μR	0.42	0.23	0.22	0.22	0.36	0.26	0.43	0.27

* Key to Symbols:
X_1 = Weight fraction of LiOH
W_s = Weight of sample
V_s = Volume of sample
D = Density of sample
μ = Linear absorption coefficient
R = Radius of sample = .159 cm

If equation (9) is solved for the sodium chloride type structure of LiH, one obtains:

$$F_{hkl} = 4 (f_{Li} \pm f_H), \qquad (19)$$

where the upper sign corresponds to structure factors for which all indices are even, and the lower sign to those with all indices odd. In both cases the structure factor is real and positive, so that the absolute value signs in equation (18) may be omitted.

From equation (18):

$$\left(I''_{T,hkl}\right)^{\frac{1}{2}} = C_T F(T,hkl)$$
$$= 4C_T (f_{Li} \pm f_H) \qquad (20)$$
$$= f'_{T,Li} \pm f'_{T,H} .$$

If one designates by $I''_{T,e}$ the value for all indices even, and by $I''_{T,o}$ the value for all indices odd, then for a given $\sin\theta/\lambda$ one finds:

$$f'_{T,Li} = \frac{1}{2}\left[(I''_{T,e})^{1/2} + (I''_{T,o})^{1/2}\right]$$
$$f'_{T,H} = \frac{1}{2}\left[(I''_{T,e})^{1/2} - (I''_{T,o})^{1/2}\right]. \qquad (21)$$

The necessary values of $(I''_{T,e})^{\frac{1}{2}}$ and $(I''_{T,o})^{\frac{1}{2}}$ were found by plotting the square roots of the corrected "intensities" against $\sin\theta/\lambda$. For each set of data, two smooth curves were drawn through the points, and from these the desired quantities were obtained at selected values of $\sin\theta/\lambda$.

The Debye-Waller expression for the temperature-dependent atomic form factor[19] is:

$$f_T = f_R e^{-M_T} = f_R e^{-B_T \frac{\sin^2\theta}{\lambda^2}} , \qquad (22)$$

where f_R, the form factor of the atom at rest, and B_T, a temperature-dependent quantity, are different for each type of atom. The quantity B_T will be discussed in greater detail later.

From equations (20) and (22):

$$\left(\frac{f'_{303}}{f'_T}\right)_{Li} = \frac{C_{303}}{C_T}\left(\frac{f_{303}}{f_T}\right)_{Li}$$

$$= \frac{C_{303}}{C_T} \exp -\left[B_{303}\left(\frac{\sin\theta_1}{\lambda}\right)^2 - B_T\left(\frac{\sin\theta_2}{\lambda}\right)^2\right] \qquad (23)$$

and similarly for the hydrogen. If the values are taken so that $\sin\theta_1 = \sin\theta_2$, then equation (23) simplifies to:

$$\left(\frac{f'_{303}}{f'_T}\right)_{Li} = \frac{C_{303}}{C_T} \exp -(B_{303} - B_T)\left(\frac{\sin\theta}{\lambda}\right)^2 \qquad (23')$$

and, taking the logarithm:

$$\ln\left(\frac{f'_{303}}{f'_T}\right)_{Li} = \ln\frac{C_{303}}{C_T} - (B_{303} - B_T)\left(\frac{\sin\theta}{\lambda}\right)^2 \qquad (24)$$

Thus an extrapolation of equation (24), which is linear in $(\sin\theta/\lambda)^2$, to $\sin\theta/\lambda$ equal to zero will give the value of $\ln\frac{C_{303}}{C_T}$ which is needed in determining the absolute atomic form factors. (See Figure 4).

For the purpose of placing the scattering factors on an absolute basis, i.e., to evaluate C_T of equation 18, a direct comparison of LiH with NaCl by substitution was made at room temperature.*

A plate of LiH cleaved parallel to a cube face was used for the measurement of the integrated reflection, ρ, of the (200) plane of LiH. In the case of NaCl, a large rock salt crystal was used, the integrated

* We are indebted to Mr. Paul D. Splitstone for carrying out this measurement.

reflection being measured by reflection from the cube face for the (200), (400), and (600) orders.

Thus:

$$\frac{\rho_{LiH}}{\rho_{NaCl}} = \frac{\left[N^2F^2 \ \frac{1+\cos^2 2\theta}{\sin 2\theta} \ e^{\frac{-\mu t}{\cos\theta}} \ \frac{t}{\cos\theta}\right]_{LiH\ (200)}}{\left[N^2F^2 \ \frac{1+\cos^2 2\theta}{\sin 2\theta} \ \frac{1}{2\mu}\right]_{NaCl\ (h00)}}$$

The values of James and Firth [20] were used for F_{NaCl} (uncorrected for extinction since no correction was made with these data). Extinction should have little effect, in any case, on the (600) reflection as shown by James and Firth's data . The values used are:

$$\frac{F_{NaCl}}{4} = 17.16\ (200),\ 11.23\ (400) \text{ and } 6.84\ (600)$$

$$\frac{\rho_{LiH\ (200)}}{\rho_{NaCl\ (200)}} = 1.20;\quad \frac{\rho_{LiH\ (200)}}{\rho_{NaCl\ (400)}} = 8.49;\quad \frac{\rho_{LiH\ (200)}}{\rho_{NaCl\ (600)}} = 21.8$$

thickness (t) of LiH plate = 0.144 cm

N = no. of unit cells per unit volume $= \frac{1}{a_o^3}$

Using the NaCl (200),(400), and (600) reflections data, F_{LiH} (200 is, respectively, 5.28, 5.72, 5.40 with an over-all average of 5.48 at room temperature).

Using the value of 5.48 as the scattering power per unit cell for the (200) reflection of LiH at 303°K, the value of C_{303} was determined. Values of C_T for the individual ions at 77° and at 20°K were then obtained from these plots.

As an alternative procedure, using an average value of the characteristic temperature, (H), of 851°(Table 5) values of f_R, the "rest"

value of the scattering factor were calculated from the values of f_{303} for both Li and H. (The values of f_{Li} and f_H were independently redetermined for this purpose by one of us from the experimental $(F_{LiH})_{303°}$ values.) Then from these values of f_R, values of $f_{77°}$ and $f_{20°}$ were calculated.

Putting

$$f_T = f_R\, e^{-B_T \frac{(h^2 + k^2 + l^2)}{4\, a^2_o}} = f_R\, e^{-B'_T (h^2 + k^2 + l^2)},$$

then

$$\left[\frac{f_T - C_T f'_T}{f_T}\right]_m = \epsilon_m, \text{ where } f'_T \text{ is the relative scattering}$$

factor (experimental) for the ion and f_T is the value as calculated above; m runs over nine values (h, k, l).

The apparent squared error ϵ_m^2 was minimized by the least squares method to yield values of C_T for both Li and H at 77° and 20° K. The values of C_T obtained in this way are compared in Table 4a with the values read from the extrapolation plots. It is clear that, within experimental error, the values are not different.

Although the data for LiD were related through experiment with the data for LiH, it is clear that these also have been correctly treated since the values of f_R for Li in LiD are practically identical with those in LiH.

TABLE 4a. PROPORTIONALITY CONSTANTS FOR CONVERTING RELATIVE FORM FACTORS TO ABSOLUTE FORM FACTORS: LiH, $(4\ C_T)^{-1}$

Temp., °K.	Least squares fit		Graphical extrapolation	
	Li	H	Li	H
20	0.0641	0.0740	0.0639	0.0704
77	0.0522	0.0650	0.0524	0.0639

TABLE 4b. PROPORTIONALITY CONSTANTS FOR CONVERTING RELATIVE FORM FACTORS TO ABSOLUTE FORM FACTORS: $(4\ C_T)^{-1}$

Temp., °K.	LiH		LiD	
	Li	H	Li	D
20	0.0639	0.0704	0.0627	0.1060
77	0.0524	0.0639	0.0408	0.0680
303	0.0503	0.0503	0.0378	0.0566

The exponent B_T in the Debye-Waller expression can be written[21]:

$$B_T = \frac{6h^2}{mk\Theta}\left\{\frac{\phi(x)}{x} + \frac{1}{4}\right\} \qquad (25)$$

where

h = Planck's constant
m = mass of atom at lattice point
k = Boltzman's constant
Θ = Debye characteristic temperature
$= \frac{h\nu_m}{k}$
ν_m = maximum frequency of elastic vibration of solid
$x = \frac{\Theta}{T}$ where T is the absolute temperature, °K.

$$\frac{\phi(x)}{x} = \frac{1}{x^2}\int_0^x \frac{\xi\, d\xi}{e^{\xi} - 1} \qquad (26)$$

The function $\phi(x)$ was evaluated numerically by Debye[22], and is tabulated in his paper for x up to 20. For larger x, Debye's equation:

$$\frac{\phi(x)}{x} = \frac{1}{x^2}\left\{\frac{\pi^2}{6} - e^{-x}(x+1) - e^{-2x}\frac{(2x+1)}{4} - \ldots\right\} \quad (27)$$

was used.

Using equation (25), the temperature dependent form factor may be written:

$$f_T = f_o \exp\left[-\frac{6h^2}{mk\textcircled{H}}\left\{\frac{\phi(x)}{x} + \frac{1}{4}\right\}\left(\frac{\sin\theta}{\lambda}\right)^2\right] \quad (22')$$

so that

$$\ln\frac{f_T}{f_{303}} = \frac{6h^2}{mk\textcircled{H}}\left\{\left(\frac{\phi(x)}{x}\right)_{303} - \left(\frac{\phi(x)}{x}\right)_T\right\}\left(\frac{\sin\theta}{\lambda}\right)^2 \quad (28)$$

By multiplying both sides by $(\lambda/\sin\theta)^2$, one obtains:

$$\frac{\lambda^2}{\sin^2\theta}\ln\frac{f_T}{f_{303}} = \frac{6h^2}{mk\textcircled{H}}\left\{\left(\frac{\phi(x)}{x}\right)_{303} - \left(\frac{\phi(x)}{x}\right)_T\right\} = \delta T \quad (29)$$

where δT is a constant for a given temperature and atom type. A plot of the functions:

$$G(\textcircled{H}) = \left(\frac{\phi(x)}{x}\right)_{303} - \left(\frac{\phi(x)}{x}\right)_T$$

$$H(\textcircled{H}) = \frac{m\,k\,\delta\,T}{6h^2} \quad \textcircled{H}$$

against $\textcircled{H}$ gives an intersection at the value of $\textcircled{H}$ corresponding to the solution of equation (29).

By this method four values of $\textcircled{H}$ for LiH and four for LiD were found (See Figure 6). These are presented in Table 5.

TABLE 4c. ABSOLUTE ATOMIC SCATTERING FACTORS FOR THE ATOMS OF LiH AND LiD

Temp., °K.	Sin θ/λ 0.25	0.30	0.35	0.40	0.45	0.50	0.55	0.60
				$f_T(Li^+)$ (LiH)				
20	1.023	0.928	0.851	0.780	0.711	0.652	0.544	0.422
77	1.021	0.922	0.838	0.780	0.713	0.644	0.534	0.414
303	1.003	0.895	0.810	0.739	0.664	0.589	0.483	0.371
				$f_T(H^-)$				
20	0.39	0.26	0.168	0.099	0.077	0.071	0.04-	0.04-
77	0.39	0.26	0.160	0.102	0.083	0.065	0.04-	0.04-
303	0.32	0.20	0.122	0.071	0.051	0.04-	0.02-	0.01
				$f_T(Li^+)$ (LiD)				
20	1.017	0.916	0.828	0.765	0.690	0.615	0.508	0.396
77	1.007	0.905	0.824	0.755	0.682	0.607	0.501	0.388
303	0.966	0.853	0.751	0.676	0.597	0.510	0.408	0.302
				$f_T(D^-)$				
20	0.53	0.39	0.22	0.148	0.116	0.102	0.061	0.061
77	0.53	0.37	0.22	0.142	0.110	0.095	0.069	0.041
303	0.45	0.30	0.171	0.095	0.067	0.061	0.020	0.016

TABLE 5. CHARACTERISTIC TEMPERATURES FOR LiH AND LiD

Temp., °K	Atom type	LiH	LiD
20	Li	850	638
	H	835	636
77	Li	863	637
	H	855	642
Average		851	638
Ubbelohde[7]		815	611

From the average characteristic temperatures, the temperature coefficients B_T of Table (6) were calculated; and from these and the absolute form factors of Table (4), the form factors for the atoms at rest were determined. (See Table (7) and figures (5a) and (5b).

TABLE 6. TEMPERATURE COEFFICIENTS, B_T IN $(kX)^2$ FOR Li, H AND D

Crystal	Atom type	Temp., °K			
		0°	20°	77°	303°
LiH	Li	0.485	0.487	0.510	0.836
	H	3.35	3.36	3.52	5.78
LiD	Li	0.648	0.653	0.710	1.38
	D	2.21	2.22	2.42	4.71

TABLE 7. AVERAGE FORM FACTORS, f_R, FOR Li, H, AND D ATOMS AT REST

Atom type		Sin θ/λ							
		0.25	0.30	0.35	0.40	0.45	0.50	0.55	0.60
LiH:	Li^+	1.055	.970	.901	.849	.788	.731	.629	.499
LiD:	Li^+	1.055	.970	.897	.849	.792	.723	.617	.499
LiH:	H^-	.467	.369	.244	.175	.162	.158	.122	.138
LiD:	H^-	.609	.467	.304	.203	.179	.179	.122	.102
Mean	H^-	.539	.418	.274	.189	.171	.169	.122	.120

The exponent B_T can also be written as[23]:

$$B_T = 8\pi^2 \overline{U_s^2} \tag{30}$$

where U_s is the component of the displacement of the atom in the direction of the normal to the 'reflecting' plane. For an isotropic crystal the total mean square displacement is related to $\overline{U_s^2}$ by the relation:

$$\overline{U^2} = 3\,\overline{U_s^2} \tag{31}$$

Hence the total root mean square displacement or amplitude of vibration of the atoms may be expressed as:

$$\sqrt{\overline{U^2}} = \left(\frac{3\,B_T}{8\pi^2}\right)^{\frac{1}{2}} \tag{32}$$

The root mean square displacements calculated by Lonsdale[15] were average values expressed by:

$$\sqrt{\overline{U^2}} = \left(\frac{\sum M_i \overline{U_i^2}}{\sum M_i}\right)^{\frac{1}{2}} \tag{33}$$

where M_i and $\overline{U_i^2}$ are the mass and mean square displacement, respectively, of the ith kind of atom.

The total root mean square displacements for the individual atoms are shown in Table 8, while Table 9 gives the average values for comparison with Lonsdale's calculated quantities.

TABLE 8. TOTAL ROOT MEAN SQUARE DISPLACEMENTS OF ATOMS OF LiH AND LiD

Crystal	Atom	Temp., °K			
		0°	20°	77°	303°
LiH	Li	.136	.136	.139	.178
	H	.356	.358	.366	.469
LiD	Li	.157	.157	.164	.229
	D	.290	.290	.303	.423

TABLE 9. AVERAGE ROOT MEAN SQUARE AMPLITUDES FOR LiH AND LiD

	Temp., °K				
Crystal	0	20	77	303	293*
LiH	.179	.180	.184	.236	.24
LiD	.195	.195	.203	.276	.29

* Lonsdale's calculated values.[8]

From the atomic form factors for the lithium and hydrogen at 20°K (Table 4b) the crystal structure factors for lithium hydride were determined by use of equation (19). With these the electron density $\rho(xoo)$ along the cell edge was calculated, using the expression[24]:

$$V\rho(x00) = \sum_{h}\sum_{k}\sum_{l}^{-\infty\ \infty} F_{hkl} \cos 2\pi hx \qquad (33)$$

Since the resulting electron density shows diffraction effects because of termination of the series,(Figure 7), it appeared desirable to extrapolate the atomic form factor curves to larger values of $\frac{\sin\theta}{\lambda}$. At the same time it was decided that the electron density of the atoms at rest would be more informative. Consequently the atomic form factor values for lithium and hydrogen in Table 7 were extrapolated according to the method of Bouman[25]. The extrapolation functions were:

$$\begin{aligned} &\text{for Li} \quad fe = 1.920 \exp 3.75\,(\sin\theta/\lambda)^2 \\ &\text{for H} \quad fe = 0.455 \exp 4.17\,(\sin\theta/\lambda)^2 \end{aligned} \qquad (34)$$

with the resulting values of F_{hkl} the electron density along the cell edge (Figure 7) was obtained.

The lowest point of the curve in Figure 7 was chosen as the boundary between the lithium and the hydrogen ions. The distance of this point from the origin (0.70 Å) is the same as that given by Wyckoff[26] for the radius of the Li ion. With the calculated electron density and the usual expression for the radial charge distribution:

$$U(r) = 4\pi r^2 \rho(r) \qquad (35)$$

the curves of Figure 8 were obtained.

The maximum in the curve for the lithium corresponding to the radius of the K shell, occurs at 0.31 Å., while a minimum in the curve for the hydrogen occurs at about 0.5 Å.

The area under the radial distribution curve (i.e., the charge per ion) for the lithium is 1.49 electrons, while that for the hydrogen is 2.00 electrons.

4. DISCUSSION OF ERRORS

The relative error in the experimentally observed counting rates varies from about one-half per cent for the largest counting rate to about five per cent for the lowest, with a mean value of approximately two per cent.

The correction for missed counts (equation 5) involves the use of an experimentally determined effective dead time which may be in error by as much as fifty per cent. However, even with this large an error, for the extreme case of the highest observed counting rate (300 cps) the relative error in the corrected counting rate due to the error in ϵ is

six per cent, while for the lowest it is one-half per cent. Thus the mean relative error arising from this cause in the areas under the peaks of the corrected curves is around two per cent.

A far more serious source of error in the "integrated intensities" (I') is the uncertainty involved in drawing the base line and resolving the peaks, as a result of the presence of impurity.

Two separate spectroscopic analyses of the materials used indicated the presence of not more than trace quantities of such impurities as sodium, calcium, aluminum, and other heavy metals.

The method used depends on crystal structure factors calculated for lithium hydroxide, which are based on not very accurately estimated parameters for the oxygen atom. Further the resolution of overlapping peaks is somewhat arbitrary. While no calculation of the resulting error is possible, it is estimated that the error in intensity estimation could amount to as much as five per cent.

The relative intensities (I") which are obtained by correcting I' for multiplicity and absorption are within a given run as accurate as the integrated intensities from which they are derived. This is true because although the absorption corrections may be in error they are essentially independent of the scattering angle for such light absorbers. However, as soon as an attempt is made to place all runs on a common basis, the magnitude of the absorption correction becomes important. In calculating the latter the factors subject to error are the density and the mass absorption coefficient of the sample. The relative error of the volume of the sample is six per cent and that of the mass is about one-tenth

per cent, so that the relative error of the density is six per cent. The correctness of the mass absorption coefficeimt depends in part on the accuracy of the composition of the samples, and since the latter is determined from the ratio of two lines on the I' plot it may be off by as much as ten per cent. Further, the experimental mass absorption coefficient for LiH as obtained by Griffith[9] was used in the calculation, and since his bricquetted powder sample probably contained lithium hydroxide (for which no allowance was made) his value is undoubtedly high by an unknown amount. The result of these factors is that the absorption correction may be in error by as much as ten per cent.

The calculation of the characteristic temperatures, the exponents B_T and the amplitudes of vibration depend on the slope of equation (24) and on the temperature at which the data were taken. Since the slope of equation (24) is independent of the magnitude of the proportionality constant, the uncertainty of the absorption correction does not affect the above quantities. The function, $G(\textcircled{H})$, used in determining $\textcircled{H}$ is temperature-dependent, and a five-degree temperature error would cause an error of four degrees in $\textcircled{H}$, an amount which is negligible compared to the two per cent error that could result from a five per cent error in the integrated intensities. Since at the temperatures for which measurement is uncertain $\varphi(x)/x$ is small compared to 1/4 (equation 25), the exponent B_T is relatively insensitive to temperature variation. A five degree error in temperature causes a negligible error in B_T, and hence in the amplitudes of vibration. Thus the primary source of error in B_T and $\overline{U^2}$ is the two per cent error possible in $\textcircled{H}$.

The error in the absolute form factors as tabulated is difficult to evaluate. The principal error should arise in the determination of the proportionality constants, C_T, and the fixing of the absolute value of one of these.

It is believed that the absolute value of C_{303} for LiH is good to ± three per cent. Further, the individual ion-values (relative) of C_T appear to be good to one per cent for the case of lithium and five per cent for the case of hydrogen.

Ahmed[10] has recently determined the values of $(F_{LiH})_{rel}$ at room temperature from a single crystal of LiH using a photographic method. His results at this temperature agree rather well with the corresponding values reported here except for the reflections (220) and (224) which appear to be too large by comparison (ca. fifteen per cent).

5. DISCUSSION OF RESULTS

It is convenient to discuss first those results which depend only on relative intensities and are independent of the method employed for placing the measurements on an absolute basis.

A significant feature of these measurements is that the $\ln(f'_{303}/f'_T)$ plots for lithium and hydrogen (Figure 4) do not extrapolate to the same point. According to Equation (18) the constant C_T for each run should be the same for the lithium as for the hydrogen. An error in drawing the base line for diffracted intensities could give rise to the crossing point noted; however, to eliminate the error would require that the base line be moved up, for which there is no justification in the appearance of the data, and in addition this would introduce curvature into the plot of $\ln(f'_{303}/f'_T)$.

The most plausible explanation appears in a reexamination of equation (23'). In this it is assumed that the form factor for the atom at rest (f_R) for the lattice at room temperature is the same as that for the lattice at temperature T. If this is not true, then equation (23) should be written as:

$$\frac{f'_{303}}{f'_T} = \frac{C_{303}(f_R)_{303}}{C_T(f_R)_T} \exp - \left[(B_{303} - B_T)(\sin \theta/\lambda)^2\right] \quad (23'')$$

(A plot of $\ln(f'_{303}/f'_T)$ would not necessarily be linear in $(\sin \theta/\lambda)^2$.)

Now a change in f_R between the two temperatures implies a change in the state of ionization of the atom concerned, so that if Z_T represents the effective charge of the ion at temperature T, then the logarithm of Equation (23'') would extrapolate to:

$$\ln \frac{C_{303}\ Z_{303}}{C_T\ \ Z_T}, \text{ since } f_T \longrightarrow Z_T \text{ as } \frac{\sin \theta}{\lambda} \longrightarrow 0.$$

Since the total charge of the cell must remain constant, an increase in Z_T for the lithium with decreasing temperature would have to occur at the expense of a corresponding decrease in Z_T for the hydrogen. Such a redistribution of charge would make the constant for the lithium smaller than that for the hydrogen, in agreement with the observed results.

Added confirmation of this conclusion appears in the fact that if the ratio f'_{77}/f'_{20} is used for the extrapolation the difference between the lithium and hydrogen constants becomes much smaller, which would imply that the change occurs between 77°K and 303°K.

One can make an estimate of the sort of charge redistribution this corresponds to: The average value of the ratio $\frac{\left(\frac{C_{303}}{C_T}\right)_{Li}}{\left(\frac{C_{303}}{C_T}\right)_{H}} = 1.14$ for both LiH and LiD at both (lower) temperatures. As was discussed before, this means that $f_{20°}$ for H multiplied by $e^{\left(\Delta(B_T)\frac{\sin^2\theta}{\lambda^2}\right)}$ gives a value too small at room temperature and vice versa for Li.

Now, since $f\left(\frac{\sin\theta}{\lambda}\right) \longrightarrow Z$ as $\frac{\sin\theta}{\lambda} \longrightarrow 0$, $\frac{\left(\frac{Z_{303}}{Z_T}\right)_{H}}{\left(\frac{Z_{303}}{Z_T}\right)_{Li}} = 1.14.$

One can proceed further if it is assumed that LiH (or LiD) is completely ionized at room temperature; that is, $Z_{Li} = Z_H = 2$ electrons. Then at T (20° or 77°), $Z_{Li} = 2 + \delta Z$, $Z_H = 2 - \delta Z$. $S = \frac{2+\delta Z}{2-\delta Z} = 1.14$; $\delta Z = 0.13$.

Thus, on these assumptions, at a sufficiently low temperature LiH and LiD are not completely ionic, but about 87% of the charge is transferred. It is not surprising that the charge transfer is about the same at 77° as at 20°K, since the values of $\overline{U^2}$ are so nearly the same and are so near their zero-point values.

The possibility of appreciable covalent bonding in LiH has been suggested by Ewing and Seitz[30]. They have estimated that for the lattice at rest the bonding should be approximately, [illegible] 35% coulombic. Ahmed[10] has interpreted his room-temperature data on LiH by extrapolation of f_{Li}, f_H:

$$f_{Li} \longrightarrow Z_{Li};\ f_H \longrightarrow Z_H \quad \text{as} \quad \frac{\sin\theta}{\lambda} \longrightarrow 0.$$

Using this extrapolation he obtains a value of Z_{Li} of 2.75 ± 0.25 electrons, (and, of course, 1.25 ± 0.25 for the hydrogen). Since the

plots of f vs sin θ/λ have a large and increasing (negative) slope in the region of small $\frac{\sin\theta}{\lambda}$, such an extrapolation is open to considerable question.

One possible explanation of the change in the state of ionization could be found in the symmetry of the lattice. For the case of the atoms at rest, each lithium atom is coordinated with six hydrogen atoms on orthogonal axes, and conversely. This condition is favorable to a resonance of covalent bonds throughout the six bonding directions. As the temperature is increased, the nuclei begin to vibrate farther from their equilibrium rest position, destroying the symmetry that favored resonance and thus favoring a shift to coulombic binding with its greater flexibility. Such a process would be compatible with the suggested increase in ionization of the atoms with increasing temperature.

There is theoretical justification for a change in the characteristic temperature[25] with the temperature of the crystal; however, its only effect on the logarithmic plots would be to introduce a curvature which was not observed. Further, the characteristic temperatures shown in Table 5 are in excellent agreement with those calculated by Ubbelohde[7] (815°K for LiH and 611°K for LiD), especially when account is taken of the fact that his values are based on specific heats, and according to James[28] the (H) calculated from x-ray measurements should be between three and five per cent higher because of a difference in the method of obtaining the mean of the maximum of frequency for the longitudinal and transverse waves. From these values of (H) and the relationship:

$$h\nu_{max} = k(H) \qquad (40)$$

one finds that the mean maximum frequencies of vibration are 1.77×10^{13} sec^{-1} for the LiH and 1.33×10^{13} sec^{-1} for the LiD. These correspond to reststrahlen wave lengths of 17 μ and 22 μ for the LiH and LiD, respectively. Thus it should be feasible to obtain a confirmation of the (H) values by infrared measurements.

The amplitudes of vibration $\sqrt{\overline{U^2}}$ agree well with Lonsdale's [8] calculations (Table 9), a not very surprising result since she used Ubbelohde's characteristic temperatures. The amplitudes for lithium and for hydrogen are in the proper ratio for their relative masses, and the change in amplitude resulting from the substitution of deuterium for hydrogen is as would be expected.

The interpretation of (H), B_T and $\overline{U^2}$ depend on the degree to which the crystal of LiH approximates the ideal model of the Debye theory. The most serious departure from this model is that, instead of a crystal of atoms of one kind, lithium hydride is a binary crystal. Hence, there may be a wide separation between the acoustic and optical vibration bands.

From the charge density determinations one obtains for the radius of the lithium ion at rest the value 0.70 angstroms, and by subtraction from the half cell-edge, the value 1.33 angstroms for the hydrogen ion at rest. By apportioning the change in half cell-edge with increasing temperature between the two ions in the ratio of their amplitudes of vibration, the ionic radius for lithium at room temperature remains 0.70 angstroms, but that for hydrogen becomes 1.34 angstroms. According to equation (22) these radii are for the atoms in the state of ionization found at room temperature. The lithium radius is in exact agreement

with that reported by Wyckoff[26] for the Li^+ ion, while the radius for the hydrogen is within six per cent of this value for the H^- ion.

The radius of the K shell for the lithium ion, as determined from the maximum of the radial charge distribution for lithium is 0.31 angstroms, which is in acceptable agreement with theoretical calculations by Wilson[29]. (His value is 0.28 angstroms.) The total charge for the lithium ion (1.49 electrons) which is determined from the integration of the radial charge distribution over (r) appears to be much too low, since a partially ionized lithium atom should have a charge of greater than two electrons.

Thus, 3.5 of the four electrons are found in the spheres drawn about the Li and H centers. Since integration of the charge density over one-fourth of the unit cell must yield just four electrons as a result of the F_{000} term in the summation, the unaccounted-for charge is in the interstitial space not covered by the spherical integration limits chosen. In any case, this integration is subject to considerable error at large values of the radius.

Considerable confidence in the absolute magnitudes of the scattering powers is contributed by the fact that the charge density ρ_{xoo} falls so nearly to zero between the lithium and the hydrogen.

Ewing and Seitz[30] calculated the charge distribution for the LiH lattice at rest using an approximate, self-consistent field method. They list no quantitative results, so it was not possible to calculate scattering factors for comparative purposes. Their U (r) for Li and H is compared with the results obtained here in Figures 8a, b. For the

purposes of comparison, since the ordinate scale was unknown, the scale has been chosen so as to give as good agreement with the U(r) of lithium as possible.

BIBLIOGRAPHY

1. Bijvoet, J. M. and Karrsen, A. Proc. Acad. Sci., Amsterdam, 25, 27 (1922).
2. Bijvoet, J. M., Rec. trav. chim., 42, 133 (1924).
3. Huttig, G. F., Zeit. f. anorg. Chem., 141, 133 (1924)
4. Bijvoet, M. M. and Frederikse, W. A., Rec. trav. chim., A5, 1041 (1929).
5. Zintl, E. and Harder, A., Zeit. f. physik, Chem., B 14, 265 (1931).
6. Zintl, E. and Harder, A., Zeit. f. physik. Chem., B 28, 478 (1935).
7. Ubbelohde, A. R., Trans. Faraday Soc., 32, 525 (1936).
8. Lonsdale, K., Acta. Cryst. 1, 142 (1948).
9. Griffith, R. L., Dissertation, Ohio State Univ. (1940).
10. Ahmed, M. S., Phil. Mag. 42, 997 (1951).
11. Van Horn, H. H., Dissertation, Ohio State Univ. (1947).
12. Kurbatov, J. D. and Mann, H. B., Phys. Rev., 68, 40 (1945).
13. Alexander, L., Kummer, E., and Klug, H., J App. Phys. 20, 735 (1949).
14. Cochran, W., Acta. Cryst., 3, 268 (1950).
15. Compton, A. H. and Allison, S. E., X-rays in Theory and Experiment, 2nd Ed., D. van Nostrand Co., N.Y. (1935), p. 417.
16. Wyckoff, R.W.E., Crystal Structure, Vol. I, Interscience Publishers, Inc., N.Y. (1948) Chap. III, text page 33 and table page 27.
17. Internalionale Taballen sur Bentimmung von Kristallstrukturen, vol. II, Berlin (1935) p. 577.

18. Int. Tab., Ref. 17, p. 584.

19. James, R. W., The Optical Principles of the Diffraction of X-rays, G. Bell and Sons, Ltd., London (1948), p. 227.

20. James, R. W. and Firth, R. M., Proc. Roy. Soc., A 117, 62 (1927).

21. James, R. W. Ref. 19, p. 219.

22. Debye, P., Ann. d. Physik, 43, 49 (1914).

23. James, R. W. Ref. 19, p. 230

24. Int. Tab. Ref. 17, p 566.

25. Bouman, J., X-ray Crystallography, North Holland Pub. Co., (1951), p. 44.

26. Wyckoff, R. W. G., The Structure of Crystals, Chem. Catalog Co., Inc., N.Y., (1931), p.192.

27. James, R. W. Ref. 19, p. 235.

28. James, R. W. Ref. 19, p. 222.

29. Wilson, W. B., J. Chem. Phys 1, 210 (1933)

30. Ewing, D. H. and Seitz, F., Phys. Rev. 50, 772 (1936).

NOTE: In submitting this report it is understood that all provisions of the contract between The Foundation and the Cooperator and pertaining to publicity of subject matter will be rigidly observed.

Investigator C. K. Stambaugh by P.M.H Date March 30, 1953

Supervisor P. M. Harris Date Mar. 30, 1953

FOR THE OHIO STATE UNIVERSITY RESEARCH FOUNDATION

Executive Director Owen C. Wolfert Date 3/30/53

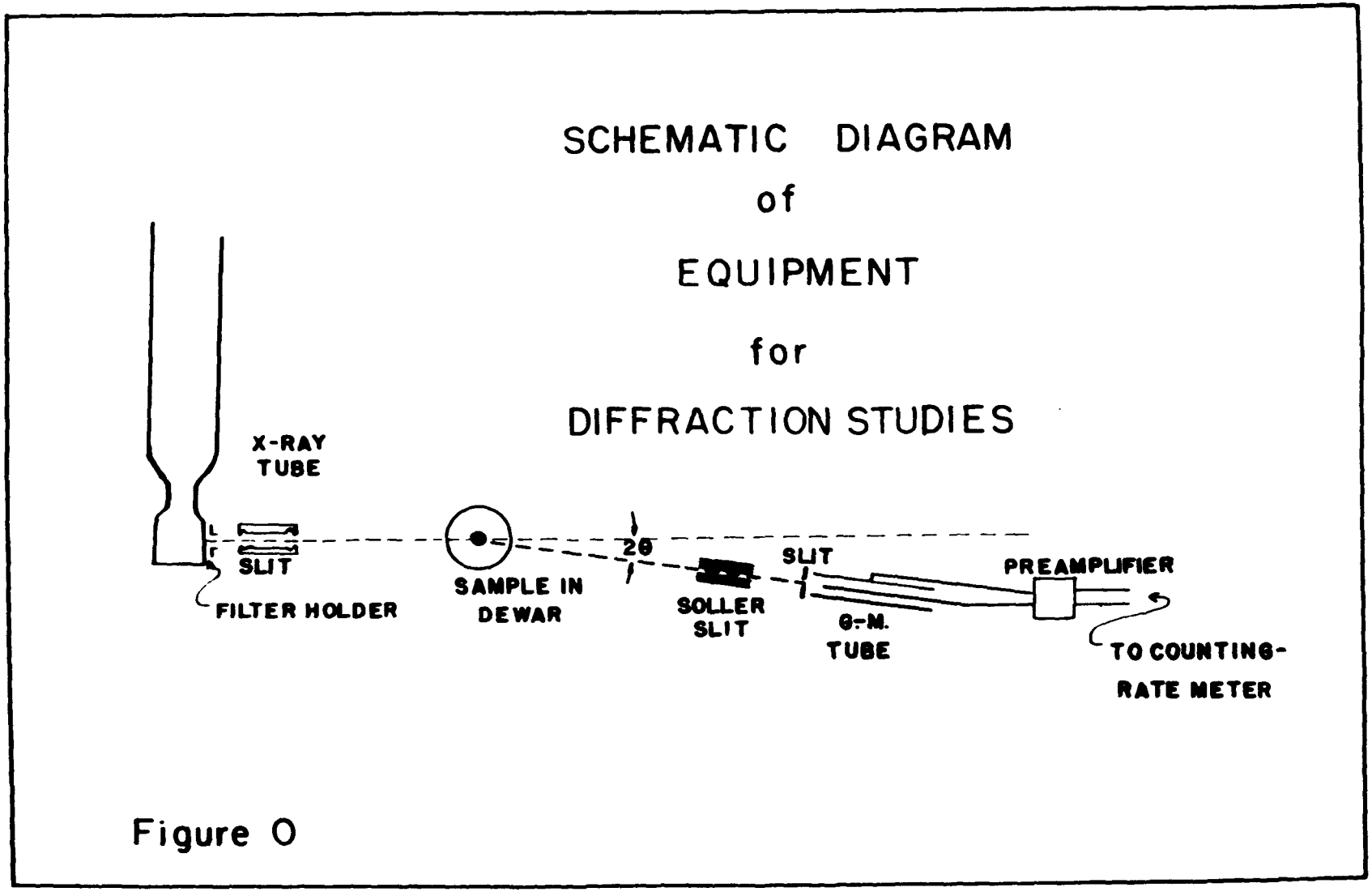
SCHEMATIC DIAGRAM
of
EQUIPMENT
for
DIFFRACTION STUDIES
X-RAY TUBE
SLIT
FILTER HOLDER
SAMPLE IN DEWAR
2θ
SOLLER SLIT
SLIT
G-M. TUBE
PREAMPLIFIER
TO COUNTING-RATE METER

Figure 0

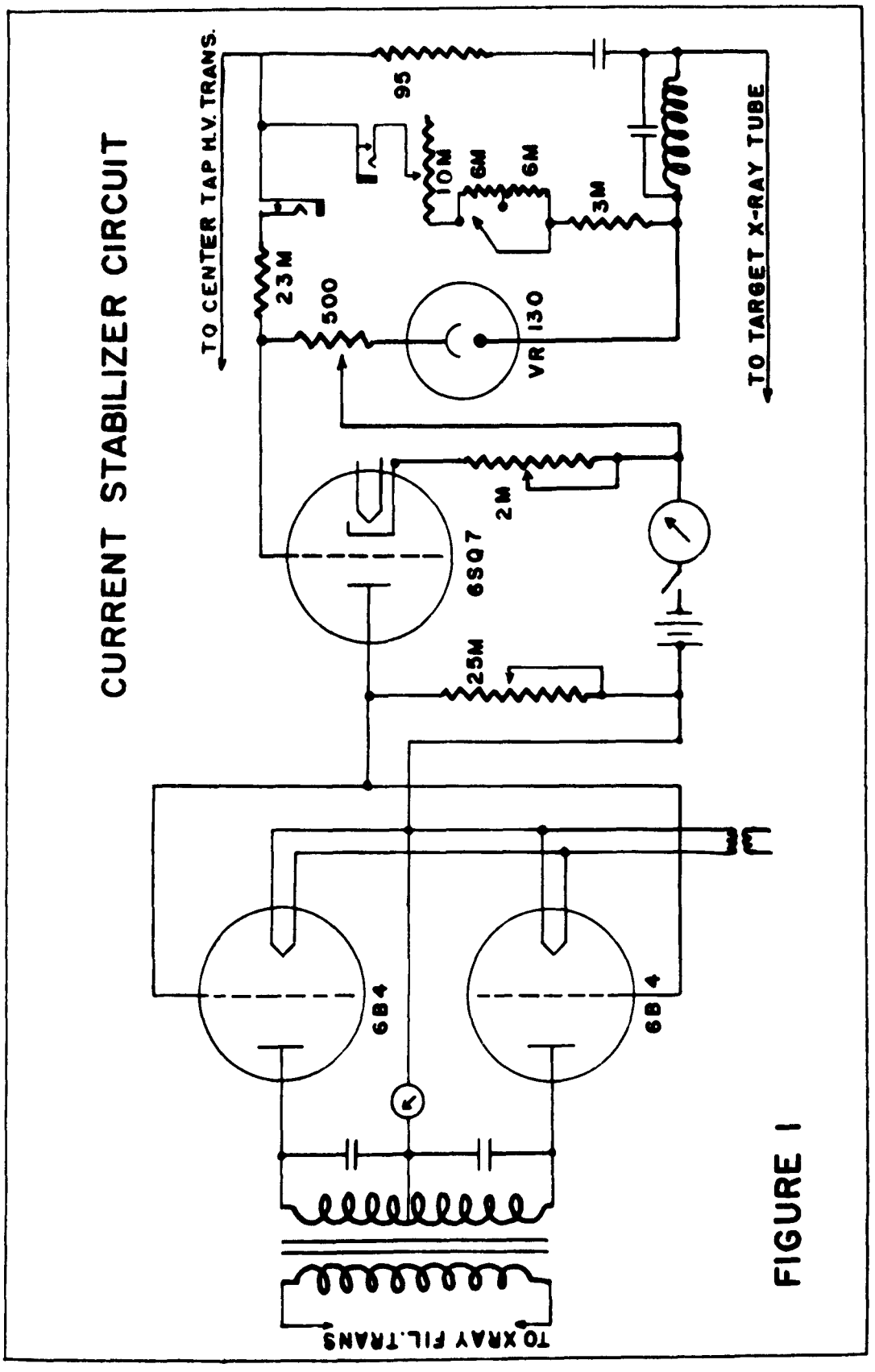
CURRENT STABILIZER CIRCUIT
TO CENTER TAP H.V. TRANS.
95
10M
6M
6M
3M
23M
500
VR 130
TO TARGET X-RAY TUBE
2M
6SQ7
25M
6B4
6B4
TO XRAY FIL. TRANS

FIGURE 1

FIGURE 2

DEWAR SPECIMEN MOUNT

FOR

LOW TEMPERATURE

DIFFRACTION

STUDIES

WITH

X-RAY SPECTROMETER

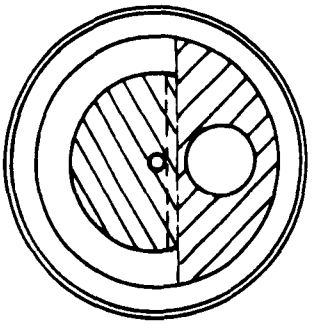

Section A-A

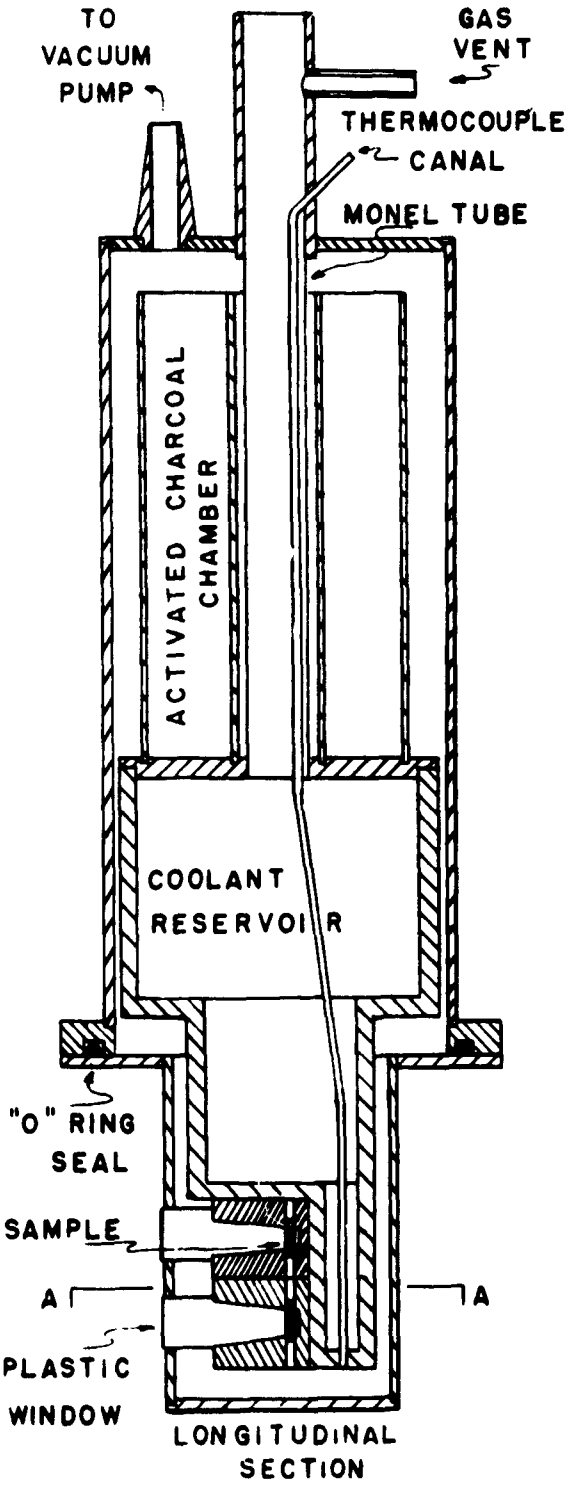

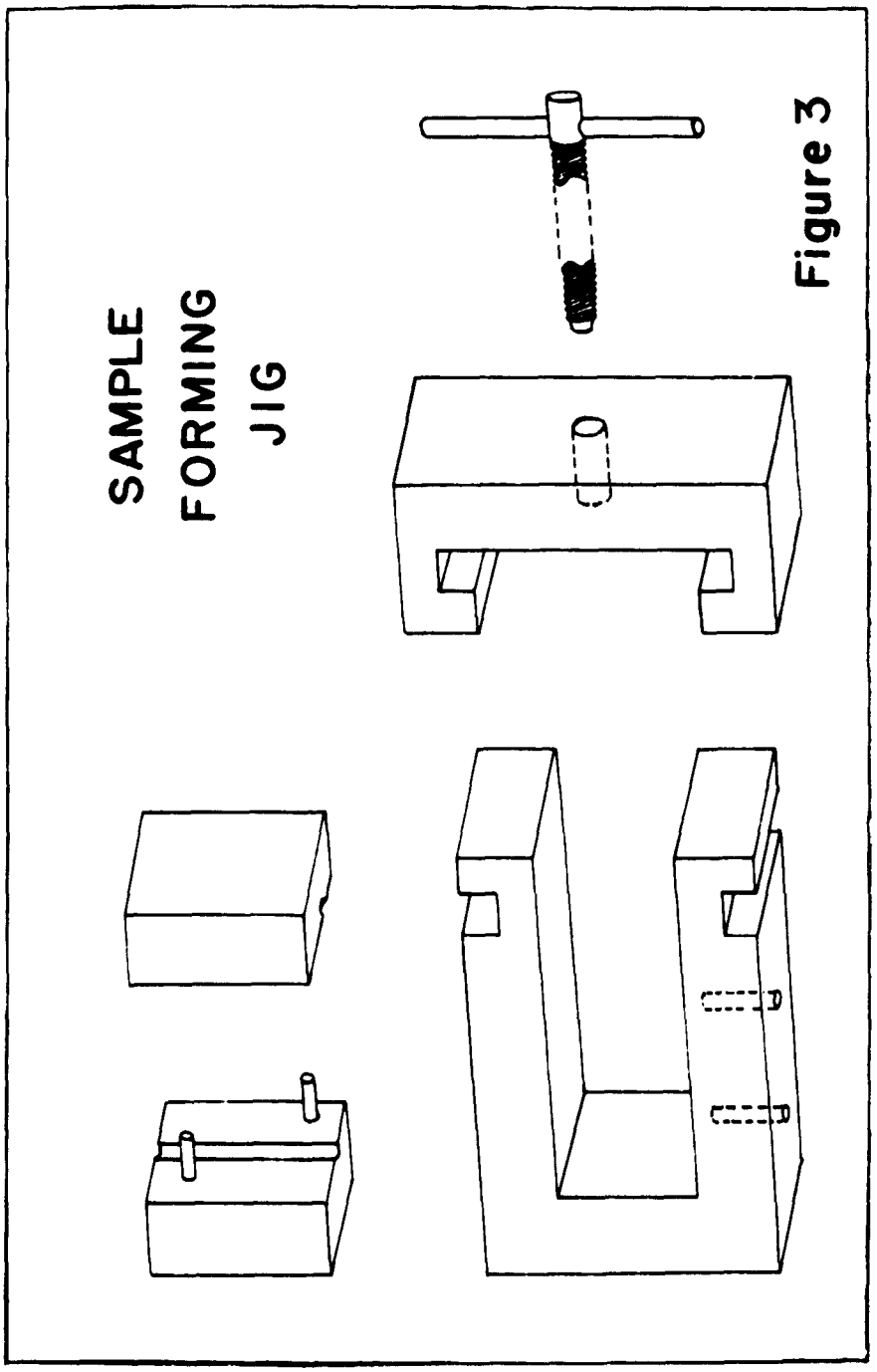

Figure 3

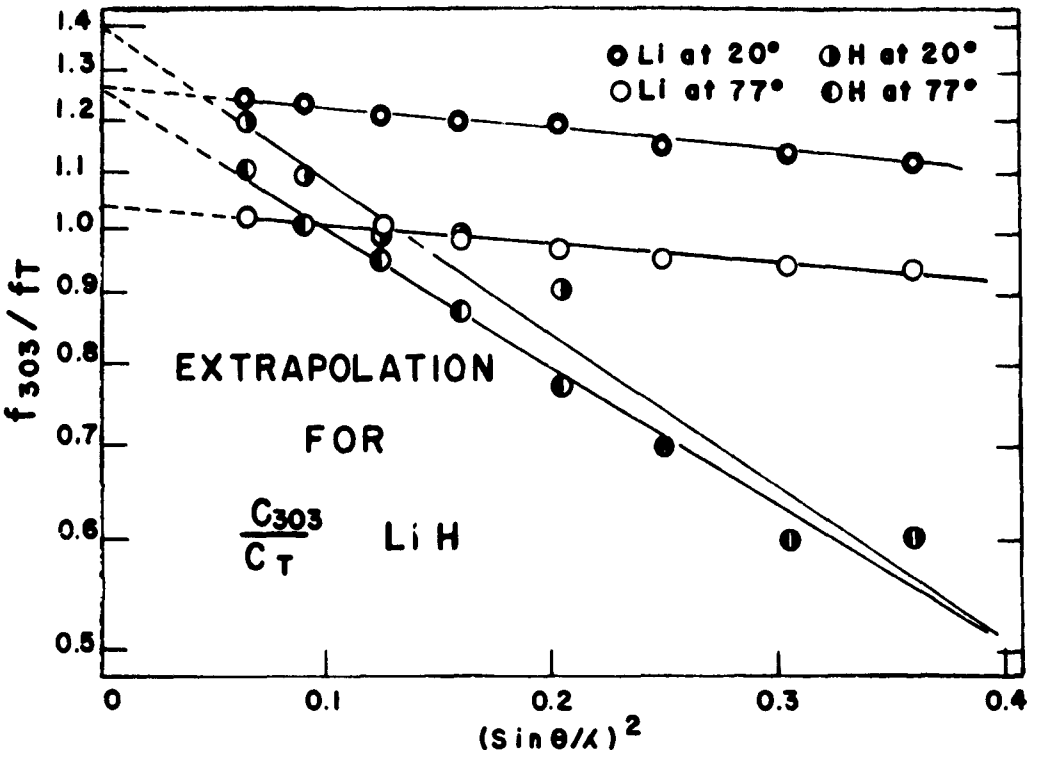
Li at 20° H at 20°
Li at 77° H at 77°
EXTRAPOLATION
FOR
$\frac{C_{303}}{C_T}$ LiH
f_{303}/f_T
$(\sin\theta/\lambda)^2$

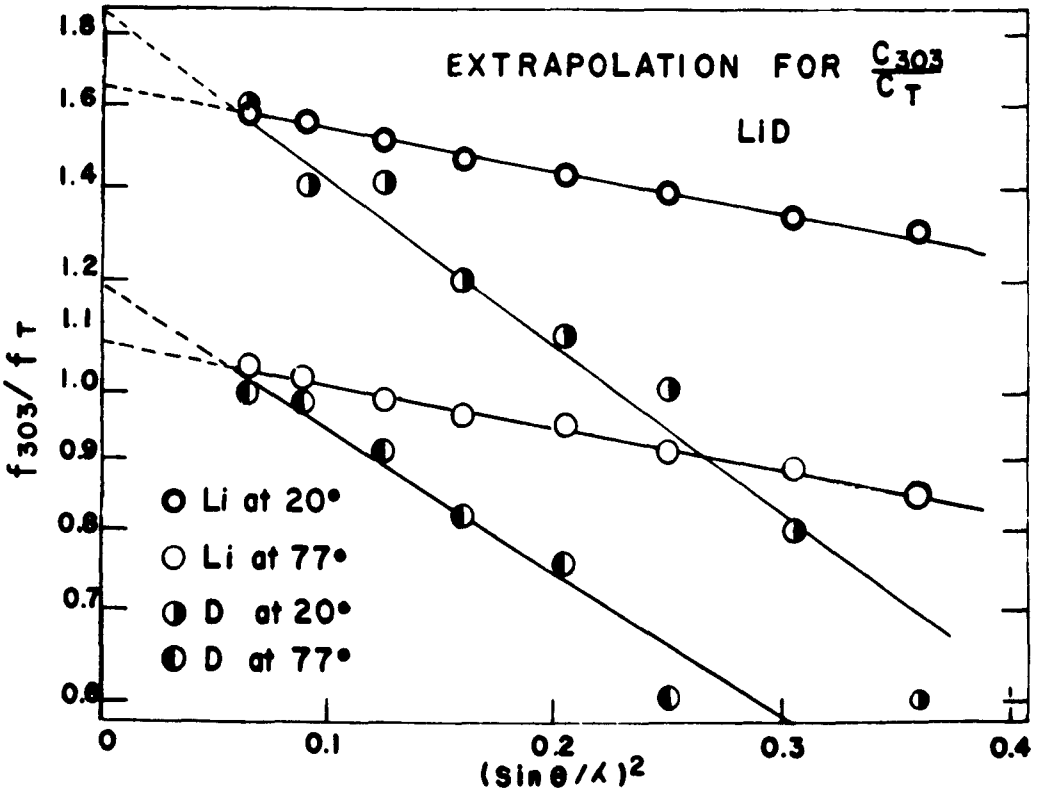
EXTRAPOLATION FOR $\frac{C_{303}}{C_T}$
LiD
Li at 20°
Li at 77°
D at 20°
D at 77°
f_{303}/f_T
$(\sin\theta/\lambda)^2$

Figure 4

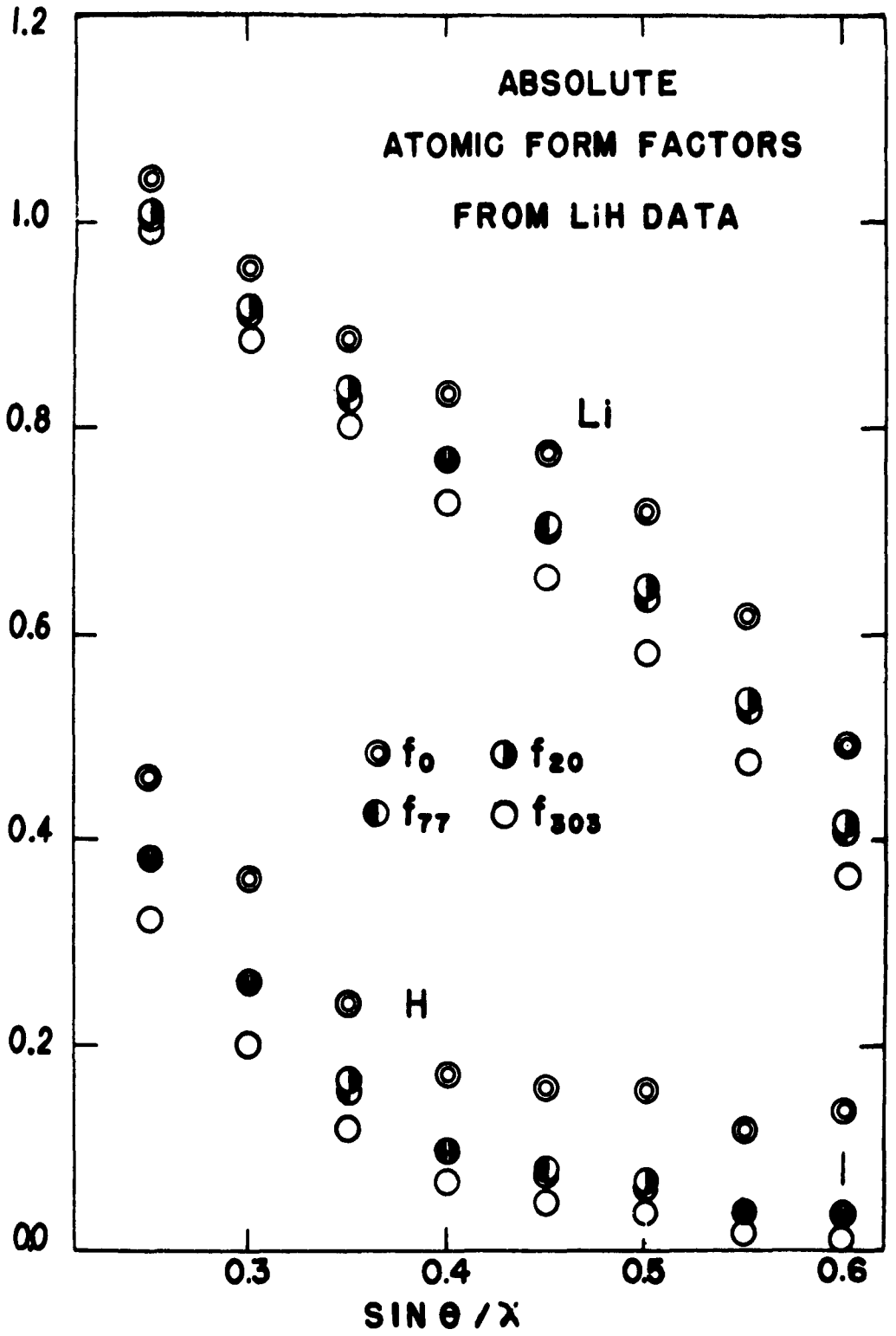
ABSOLUTE
ATOMIC FORM FACTORS
FROM LiH DATA
Li
H
f_0
f_{20}
f_{77}
f_{303}
1.2
1.0
0.8
0.6
0.4
0.2
0.0
0.3
0.4
0.5
0.6
SIN θ / λ

Figure 5a

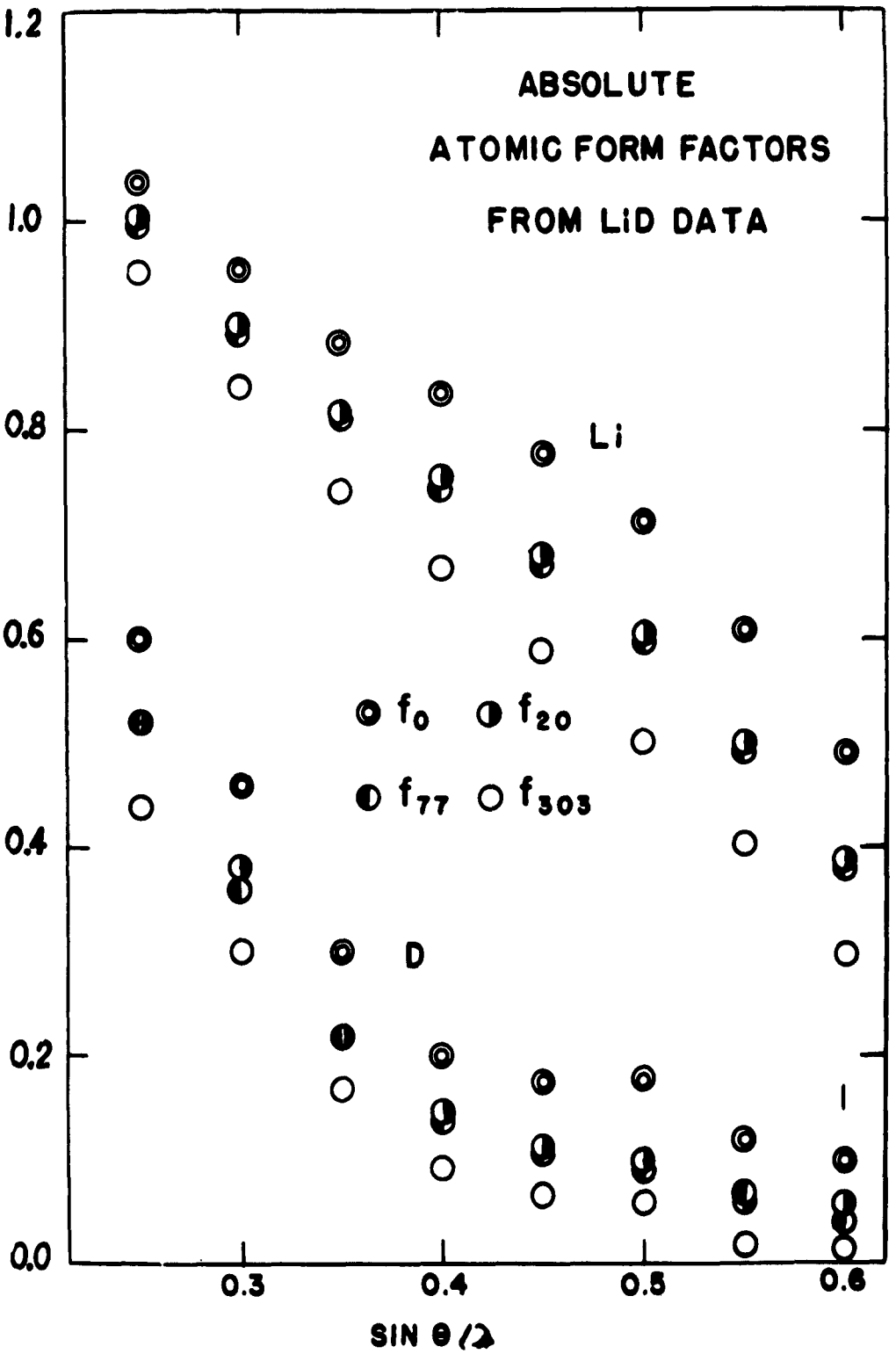
ABSOLUTE
ATOMIC FORM FACTORS
FROM LiD DATA
Li
D
I
f_0
f_{20}
f_{77}
f_{303}
1.2
1.0
0.8
0.6
0.4
0.2
0.0
0.3
0.4
0.5
0.6
SIN θ/λ

Figure 5b

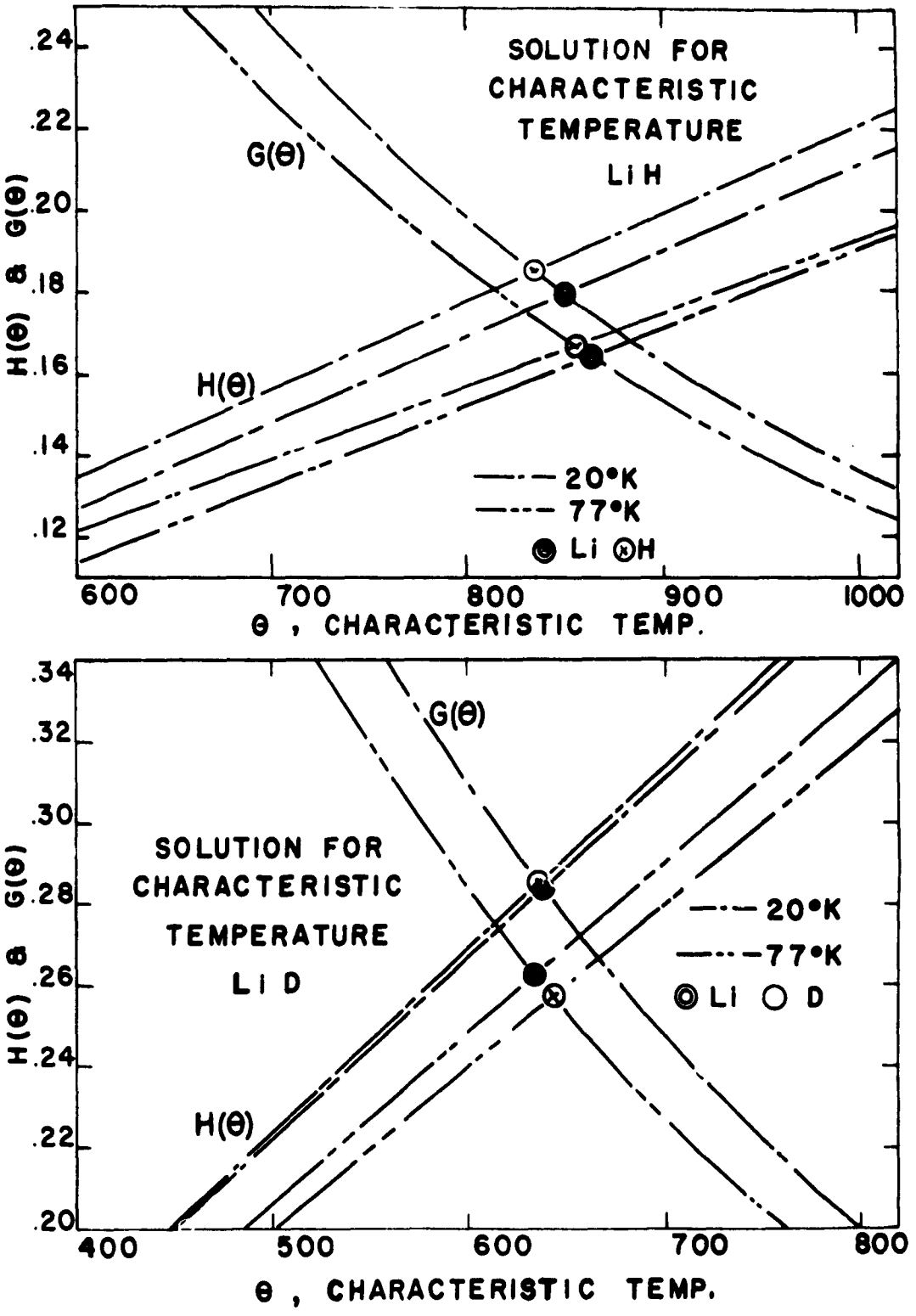
SOLUTION FOR
CHARACTERISTIC
TEMPERATURE
LiH
G(θ)
H(θ)
20°K
77°K
Li ⊗H
H(θ) & G(θ)
θ , CHARACTERISTIC TEMP.
SOLUTION FOR
CHARACTERISTIC
TEMPERATURE
LiD
G(θ)
H(θ)
20°K
77°K
Li ○ D
H(θ) & G(θ)
θ , CHARACTERISTIC TEMP.

Figure 6

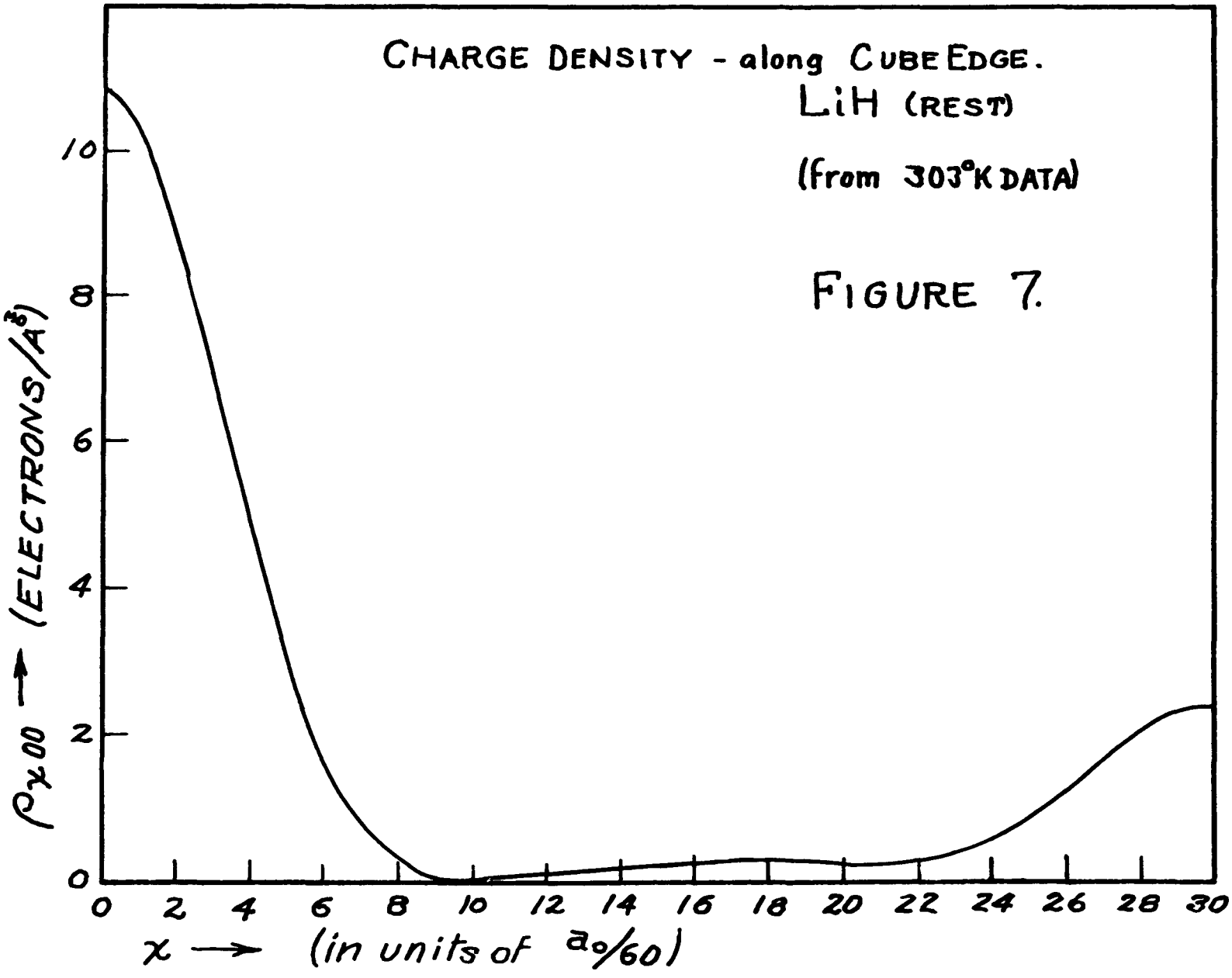
CHARGE DENSITY - along CUBE EDGE.
LiH (REST)
(from 303°K DATA)
FIGURE 7.
ρ_{x00} → (ELECTRONS/A°)
0
2
4
6
8
10
0 2 4 6 8 10 12 14 16 18 20 22 24 26 28 30
x → (in units of $a_0/60$)

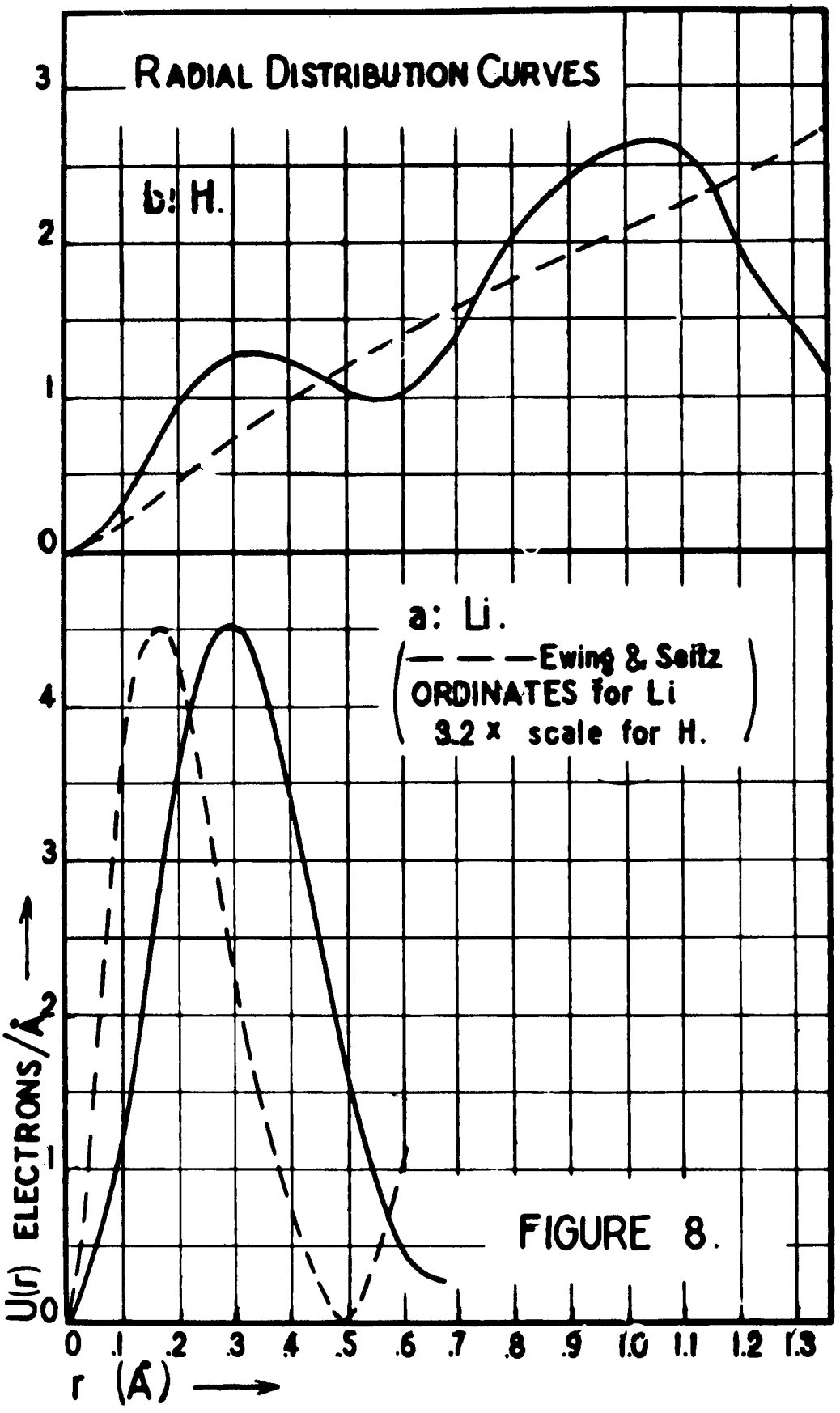
RADIAL DISTRIBUTION CURVES
b: H.
a: Li.
(— — —Ewing & Seitz ORDINATES for Li 3.2 x scale for H.)
FIGURE 8.
U(r) ELECTRONS/Å
r (Å)
0 .1 .2 .3 .4 .5 .6 .7 .8 .9 1.0 1.1 1.2 1.3
0 1 2 3 4